

Discovery of Three-Jet Events and a Test of Quantum Chromodynamics at PETRA

D. P. Barber, U. Becker, H. Benda, A. Boehm, J. G. Branson, J. Bron, D. Buikman, J. Burger, C. C. Chang, H. S. Chen, M. Chen, C. P. Cheng, Y. S. Chu, R. Clare, P. Duinker, G. Y. Fang, H. Fesefeldt, D. Fong, M. Fukushima, J. C. Guo, A. Hariri, G. Hertel, M. C. Ho, H. K. Hsu, T. T. Hsu, R. W. Kadel, W. Krenz, J. Li, Q. Z. Li, M. Lu, D. Luckey, D. A. Ma, C. M. Ma, G. G. Massaro, T. Matsuda, H. Newman, J. Paradiso, F. P. Poschmann, J. P. Revol, M. Rohde, H. Rykaczewski, K. Sinram, H. W. Tang, L. G. Tang, Samuel C. C. Ting, K. L. Tung, F. Vannucci, X. R. Wang, P. S. Wei, M. White, G. H. Wu, T. W. Wu, J. P. Xi, P. C. Yang, X. H. Yu, N. L. Zhang, and R. Y. Zhu

III. Physikalisches Institut Technische Hochschule, Aachen, West Germany, and Deutsches Elektronen-Synchrotron (DESY), Hamburg, West Germany, and Laboratory for Nuclear Science, Massachusetts Institute of Technology, Cambridge, Massachusetts, and National Instituut voor Kernfysica en Hoge-Energiefysica (NIKHEF), Sectie H, Amsterdam, The Netherlands, and Institute of High Energy Physics, Chinese Academy of Science, Peking, People's Republic of China

(Received 31 August 1979)

We report the analysis of the spatial energy distribution of data for $e^+e^- \rightarrow$ hadrons obtained with the MARK-J detector at PETRA. We define the quantity "oblateness" to describe the flat shape of the energy configuration and the three-jet structure which is unambiguously observed for the first time. Our data can be explained by quantum chromodynamic predictions for the production of quark-antiquark pairs accompanied by hard noncollinear gluons.

In previous papers¹ we have reported the observation of a two-jet structure in the production of multihadronic states in e^+e^- annihilation at PETRA, in terms of thrust and sphericity. At higher energies, the hadrons in each jet become increasingly collimated, and the identification of these hadrons with jets becomes increasingly unambiguous. Detailed analysis of the distribution of hadronic energy in three dimensions therefore can be done in order to see the effects of quantum chromodynamics (QCD), and, in particular, the emission of gluons.

The detector we used, known as MARK-J,¹ measures the energy distribution of both neutral and charged particles (except neutrinos). It covers a solid angle of $\varphi = 2\pi$ and $\theta = 9^\circ$ to 171° (θ is the polar and φ is the azimuthal angle). Lucite Čerenkov counters surround the intersection region, followed by two layers (A and B) of three radiation lengths each of lead-scintillator shower counters, with one fast photomultiplier tube at each end. The counters A and B enable us to locate shower maxima in various θ and φ directions. They are followed by the sixteen C counters, consisting of twelve layers (twelve radiation lengths) of lead-scintillator sandwich also with one phototube at each end. Surrounding the electromagnetic shower counters are drift chambers which measure tracks from hadron showers and incident muon angle. The next layers are hadron calorimeters consisting of magnetized-iron-scin-

tillator sandwiches. The last layer of calorimeter, composed of the D counters, is used for triggering on muons and for rejecting cosmic rays. The magnetic field in the iron is toroidal and its value is 17 kG. Finally, in the outermost layer there are drift chambers which are used to measure single- and double-muon exit angles and momenta.

In the small-angle region there are four layers of scintillation counters sandwiched between 10-cm-thick iron plates to measure shower energy in the region $12^\circ < \theta < 30^\circ$.

The total energy of each interaction and the direction of a particle or group of particles is computed from the time and pulse-height information of the shower counters and calorimeter counters. The azimuthal position is determined by the finely segmented shower counters. This method enables us to determine the θ and φ angles to an accuracy of $< 5^\circ$ for e or γ and $< 15^\circ$ for hadrons.

The jet analysis of the hadronic events was performed with use of the spatial distribution of the energy deposited in the detector. For each counter hit, a vector \vec{E}^i (the energy flow) is constructed, whose direction is given by the position of the signal in the counter, and magnitude by the corresponding deposited energy. To describe the energy distribution, three orthogonal axes are defined for each event as follows:

(1) The thrust axis, \vec{e}_1 , is defined as the direction along which the projected energy flow is

maximized. The thrust, F_{thrust} and \vec{e}_1 are given by

$$F_{\text{thrust}} = \max \frac{\sum_i |\vec{E}^i \cdot \vec{e}_1|}{\sum_i |\vec{E}^i|},$$

where \vec{E}^i is the energy flow detected by a counter as described above and $\sum_i |\vec{E}^i|$ is the total visible energy of the event (E_{vis}).

(2) To investigate the energy distribution in the plane perpendicular to the thrust axis, a second direction, \vec{e}_2 , is defined perpendicular to \vec{e}_1 . It is the direction along which the projected energy flow in that plane is maximized. The quantity F_{major} and \vec{e}_2 are given by

$$F_{\text{major}} = \max \frac{\sum_i |\vec{E}^i \cdot \vec{e}_2|}{E_{\text{vis}}}; \quad \vec{e}_2 \perp \vec{e}_1.$$

(3) The third axis, \vec{e}_3 , is orthogonal to both the thrust and the major axes. It is found that the absolute sum of the projected energy flow along this direction, called F_{minor} , is very close to the minimum of the projected energy flow along any axis, i.e.,

$$F_{\text{minor}} \sim \min \frac{\sum_i |\vec{E}^i \cdot \vec{e}_3|}{E_{\text{vis}}}.$$

If hadrons were produced according to phase-space or a $q\bar{q}$ two-jet distribution, then the energy distribution in the plane as defined by the major and minor axes would be isotropic, and the difference between F_{major} and F_{minor} would be small. Alternatively, if hadrons were produced via three-body intermediate states such as $q\bar{q}g$, and if each of the three bodies fragments into a jet of particles with $\langle P_{\perp} \rangle \sim 325$ MeV, the energy distribution of these events would be oblate. The quantity oblateness, O , is defined as

$$O = F_{\text{major}} - F_{\text{minor}}.$$

The oblateness is $\sim 2\langle P_{\perp} \rangle_{\text{gluon}}/\sqrt{s}$ for three-jet final states and is approximately zero for final states coming from a two-jet distribution. According to QCD,² oblateness should increase at higher energies and at lower thrust values. The quantity oblateness is particularly suited to display the effect of gluon emission because it is rather insensitive to the detailed assumptions of QCD, such as the precise P_{\perp} distribution of the hadrons and the fragmentation functions.³

Figure 1(a) shows the measured energy dependence of the average oblateness as compared to the prediction of the $q\bar{q}g$ model² as well as the $q\bar{q}$ model. We see that at low energies, the data are in agreement with both models, while at higher

energies, $27.4 \leq \sqrt{s} \leq 32$ GeV, the data agree with the $q\bar{q}g$ calculation, and are quite inconsistent with the naive $q\bar{q}$ predictions. This is expected in QCD since more and more hard gluons are emitted as energy increases.

To check the dependence of oblateness on the P_{\perp} distribution of the hadrons and the behavior of the fragmentation function $D(Z)$ we have calculated, at $\sqrt{s} = 30$ GeV, the change in the average oblateness, $\langle O \rangle$, by changing the $\langle P_{\perp} \rangle$ from the commonly used value of 325 MeV to $\langle P_{\perp} \rangle = 425$ MeV, or by changing $D(Z) = (1-Z)^2$ with $Z = P_h/P_q$ to $D(Z) = \text{const}$ for the c (charmed) and b (bottom) quarks.⁴ In both cases $\langle O \rangle$ changes by 0.002 ± 0.002 .

Figure 1(b) shows the measured oblateness versus thrust for the combined data at $\sqrt{s} = 27.4, 30$, and 31.6 GeV. We see that for lower values of thrust the oblateness of the energy distribution

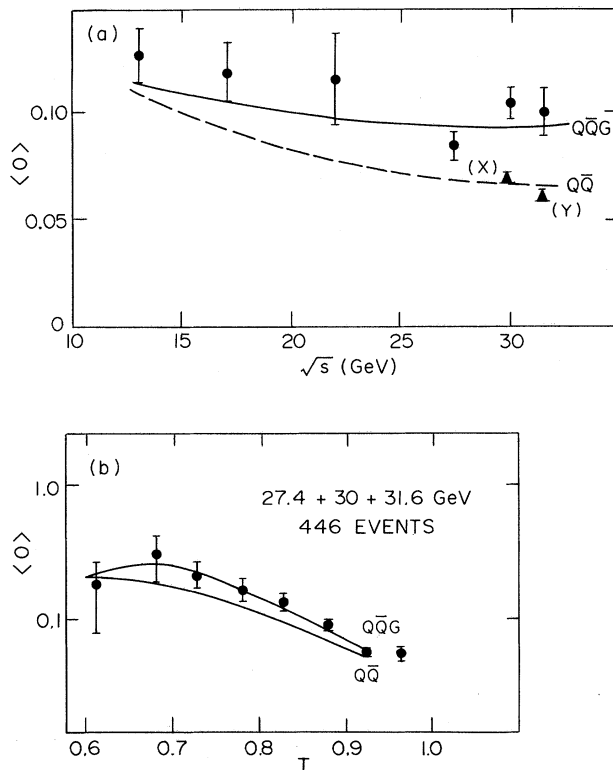


FIG. 1. (a) The average oblateness, $\langle O \rangle$, as function of \sqrt{s} compared with the predictions of $q\bar{q}$ (dashed curve) and $q\bar{q}g$ model (solid curve). Also shown are points in the $q\bar{q}$ model calculation under two different conditions: Point X: $\langle P_{\perp} \rangle = 425$ MeV, $\sqrt{s} = 30$ GeV, $D(Z) = (1-Z)^2$; point Y: $\langle P_{\perp} \rangle = 325$ MeV, $\sqrt{s} = 31.6$ GeV, $D(Z) = \text{const}$ for b and c quarks. (b) The average oblateness at 27.4–31.6 GeV as a function of thrust compared with the predictions of $q\bar{q}$ and $q\bar{q}g$ model.

increases.

Figure 2(a) shows the event distribution as a function of oblateness for the data at $\sqrt{s} = 17$ GeV where the gluon-emission effect is expected to be small. The data indeed agree with both models, although the prediction with gluons is still pre-

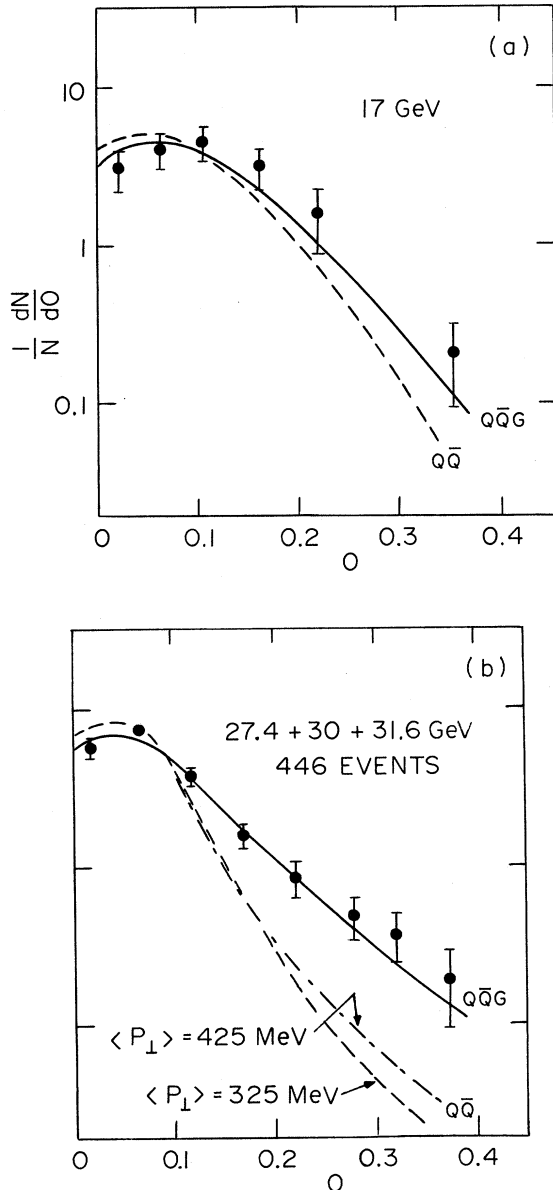


FIG. 2. (a) The distribution $N^{-1}dN/dO$ as function of oblateness at $\sqrt{s} = 17$ GeV. (b) The distribution $N^{-1}dN/dO$ as function of oblateness at $\sqrt{s} = 27.4-31.6$ GeV. In both (a) and (b) the solid curves are the predictions based on the $q\bar{q}g$ model and the dashed curve is based on the standard $q\bar{q}$ model with $\langle P_{\perp} \rangle = 325$ MeV. The dash-dotted curve in (b) is the $q\bar{q}$ model prediction with $\langle P_{\perp} \rangle = 425$ MeV.

ferred.

Figure 2(b) shows the event distribution as a function of oblateness for the data at $27.4 \leq \sqrt{s} \leq 31.6$ GeV as compared with the predictions of $q\bar{q}g$ and $q\bar{q}$ models. Again, in the $q\bar{q}$ model we use both $\langle P_{\perp} \rangle = 325$ MeV and $\langle P_{\perp} \rangle = 425$ MeV. The data have more oblate events than the $q\bar{q}$ model predicts, but they agree with the $q\bar{q}g$ model very well.

To see the detailed structure of the jets we further divide the energy distribution of each event into two hemispheres using a plane defined by the major and minor axes. The forward hemisphere contains the narrow jet and the other contains the broader jet. F_{major} , F_{minor} , and O are calculated separately for each hemisphere.

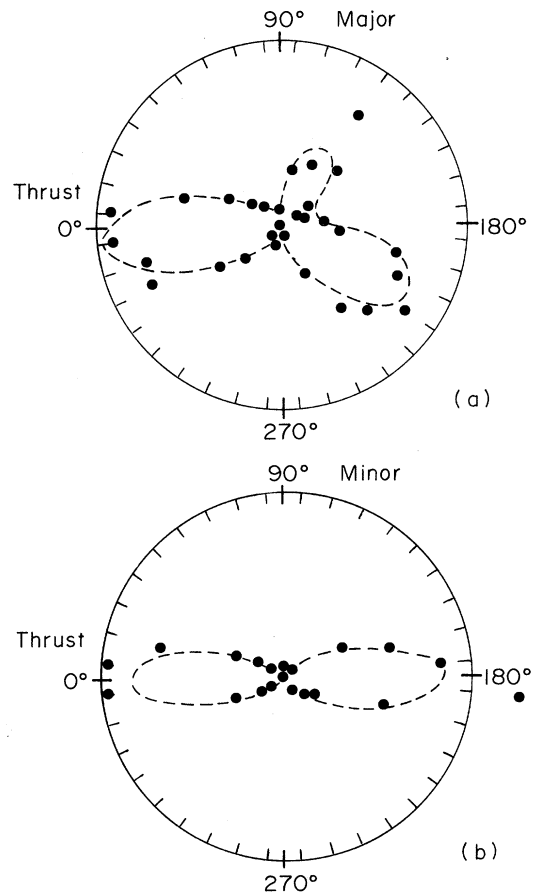


FIG. 3. (a) Energy distribution in the plane as defined by the thrust and the major axes for all the events with thrust < 0.8 and oblateness > 0.1 at $\sqrt{s} = 27.4, 30,$ and 31.6 GeV. The energy value is proportional to the radial distances. The superimposed dashed line represents the distribution calculated with use of the $q\bar{q}g$ model. (b) The measured and calculated energy distribution in the plane as defined by the thrust and the minor axes.

A sample of the events with low thrust and high oblateness, where the gluon-emission effect is expected to be relatively large, is selected for detailed examination. The sum of the angular energy distribution of all the events at $\sqrt{s}=27.4, 30,$ and 31.6 GeV with the thrust <0.8 and the oblateness of the broad jet >0.1 is shown in Figs. 3(a) and 3(b). We see in Fig. 3(a) the accumulated energy distribution in the plane defined by the thrust and major axes showing three distinct jets which up to now had not been observed.⁵ The longest jet is pointing along the thrust axis and the opposite hemisphere actually contains two smaller jets with a large angle between them. We have oriented the two small jets according to their sizes.⁶ The calculated energy distributions using the $q\bar{q}g$ model are shown in Figs. 3(a) and 3(b) and are compatible with the data with χ^2 of 67 for 70 degrees of freedom. In Fig. 3(b) we show the accumulated energy distribution in the plane defined by the thrust and minor axes, the flat distribution is again consistent with the $q\bar{q}g$ predictions.

In conclusion, we have shown that the energy flow of hadronic events from e^+e^- interactions can be described in terms of QCD. The effects are particularly striking when the data are expressed in terms of the quantity "oblateness." The average oblateness as a function of thrust and \sqrt{s} , and the differential oblateness distribution, all favor models including gluon emission. The effect clearly increases with increasing energy. The energy distribution of the events with thrust <0.8 and oblateness >0.1 shows three distinct jet structures.

We wish to thank Professor H. Schopper, Pro-

fessor G. Voss, Professor H. Feshbach, Professor E. Lohrmann, Professor F. Low, Dr. F. J. Epling, and Dr. G. Söhngen for their valuable advice and support and Dr. A. Ali and Professor H. Georgi for helpful discussions. We also thank Miss I. Schulz, Miss S. Marks, Mrs. S. Burger, Mr. P. Berges, and Mr. D. Osborne for technical and administrative help.

¹D. P. Barber *et al.*, Phys. Rev. Lett. **42**, 1110 (1979); D. P. Barber *et al.*, Phys. Rev. Lett. (to be published). Also, D. P. Barber *et al.*, Massachusetts Institute of Technology, Laboratory for Nuclear Science Report No. 104, 1979 (to be published).

²J. Ellis *et al.*, Nucl. Phys. **B111**, 253 (1976); T. DeGrand *et al.*, Phys. Rev. D **16**, 3251 (1977); G. Kramer *et al.*, Phys. Lett. **79B**, 249 (1978); A. De Rújula *et al.*, Nucl. Phys. **B138**, 387 (1978); P. Hoyer *et al.*, DESY Report No. 79/21 (unpublished); A. Ali *et al.*, DESY Report No. 79/12 (unpublished).

³H. Georgi, private communication.

⁴We have adopted the notation that Z equals a fraction of quark energy carried away by the hadron.

⁵Phase-space distribution will show three nearly identical lobes due to the method of selection used. However, at $\sqrt{s}=30$ GeV these lobes are very different in appearance from the jets shown in Fig. 3. In general, one expects the three jets from $q\bar{q}g$ to become slimmer and easier to distinguish from the phase-space distribution as the center-of-mass energy increases. Using a χ^2 fit of the phase-space energy distribution to the data we found that $\chi^2=222$ for 70 degrees of freedom. Therefore, the phase space is inconsistent with the data. Furthermore, large contributions of phase-space distributions are ruled out by our data on thrust distribution (see Ref. 1).

⁶In general the smallest jet came from gluon fragmentation.